

In situ measurements of gas-particle partitioning of organic compounds in Fairbanks

Amna Ijaz¹, Brice Temime-Roussel¹, Julien Kammer¹, Jingqiu Mao², William Simpson², Kathy Law³, Barbara D'Anna¹

¹Aix-Marseille Université, CNRS, LCE, Marseille, France

²Now at: Pacific Northwest National Laboratory, Richland, WA 99352, United States

³Department of Chemistry and Biochemistry and Geophysical Institute, University of Alaska, Fairbanks, AK, United States

⁴Sorbonne Université, UVSQ, CNRS, LATMOS-IPSL, Paris, France

Supplementary Information

S1. Data processing for correction of instrumental artefacts

The PTR ToF MS was switched between sampling the gas phase and aerosol particles via the CHARON inlet. A small amount of sample may linger in the sampling systems as they are switched to the other phase causing an overestimation in subsequent measurements, manifesting the so-called memory effect (ME) ¹. In the ALPACA campaign, gas-phase species of $m/z < 50$ were overestimated in the particle phase, while species of $m/z > 200$ were overestimated in the gas phase. Although the start and end of measurements in each sampling mode were omitted to overcome the ME, it remained an issue in the gas phase as demonstrated in **Figure S2A**, where there is a sharp decline in the F_p at $m/z > 200$ that does not align with the F_p distribution trend of the rest of the dataset. Assuming that many of these ions were unlikely to be associated very strongly with the gas phase, we applied an ME correction as demonstrated in **Figure S2B–C**. Despite the ME correction, large alkyl moieties (i.e., m/z 369.36, $C_{27}H_{44}$; m/z 399.37, $C_{29}H_{50}$; m/z 425.38, $C_{31}H_{52}$) remained in trace amounts, i.e., $<0.1\%$ of the total gas-phase mass (**Figure 1**), whose origin and appropriate reduction procedures need to be considered in detail in future studies.

S2. Details on the parameterisation of saturation mass concentrations

The VolCalc() package ² was used to estimate the C^0 using tentative identities of ions. First, the VolCalc() estimates the $\log_{10}P_i$ (i.e., \log_{10} of the vapour pressure of ion i) by implementing the SIMPOL group-contribution method as expressed in **Equation S1**, where $v_{k,i}$ is the sum of the counts of functional groups in ion i and b_k is the coefficient for each functional group ³. This vapour pressure is then used to calculate the volatility using **Equation S2** ^{4,5}, where P_i is the estimated equilibrium saturation vapour pressure for ion i , M_i is the molecular weight of i , R is the universal gas constant, and T is the standard temperature, which is set by default to 293 K in VolCalc(). The activity coefficient (γ_i) was assumed to be 1. The elemental composition-based parameterisation ⁶ estimated volatility at 298 K using the number of C, H, O, N, and S as expressed in **Equation S3**, where the values of coefficients (i.e., n_0C , b_C , b_O , b_H , b_{CO} , b_N , and b_S) can be found in the supplement of ref. ⁶. As shown in **Figure S3**, the two methods to estimate C^0 agreed well for our dataset, except for some larger molecules ($m/z > 200$), where the elemental composition-based method estimated slightly higher C^0 on average. For this study, we have presented the results from SIMPOL-driven estimation, considering that it presented a better estimate of the volatilities of well-known compounds, such as levoglucosan (placed as an LVOC in SIMPOL-driven method, rather than an SVOC in the elemental composition-based estimation). The phase state ratio (PSR) was calculated to supplement our findings using the method of ⁷ and ⁸.

Temperature dependence of C^0 , i.e., its conversion to C^0 at measured temperatures in Fairbanks, was explored by the Clausius-Clapeyron equation ⁹ (**Equation S4**), where ΔH_{vap} is the enthalpy of vapourisation estimated for each ion from the ACD/Labs entry in ChemSpider database ¹⁰; it represents the energy required to convert a compound from liquid to gas state ¹¹. R is the universal gas constant.

$$\log_{10}P_i = \sum_k v_{k,i} \cdot b_k \quad \text{.....Equation S1}$$

$$\log_{10}C^0 = \log_{10}\left(\frac{P_i \times M_i \times \gamma_i}{R \times T}\right) \quad \text{.....Equation S2}$$

$$\log_{10}C^0 = (n_C^0 - n_C)b_C - n_Ob_O - n_Hb_H - 2\left(\frac{n_Cn_O}{n_C + n_O}\right)b_{CO} - n_Nb_N - n_Sb_S \quad \text{.....Equation S3}$$

$$C^0(at T_{meas}) = C^0(at T_{standard}) \times \exp\left(\frac{\Delta H_{vap}}{R} \times \left(\frac{1}{T_{standard}} - \frac{1}{T_{meas}}\right)\right) \dots \text{Equation S4}$$

Figures

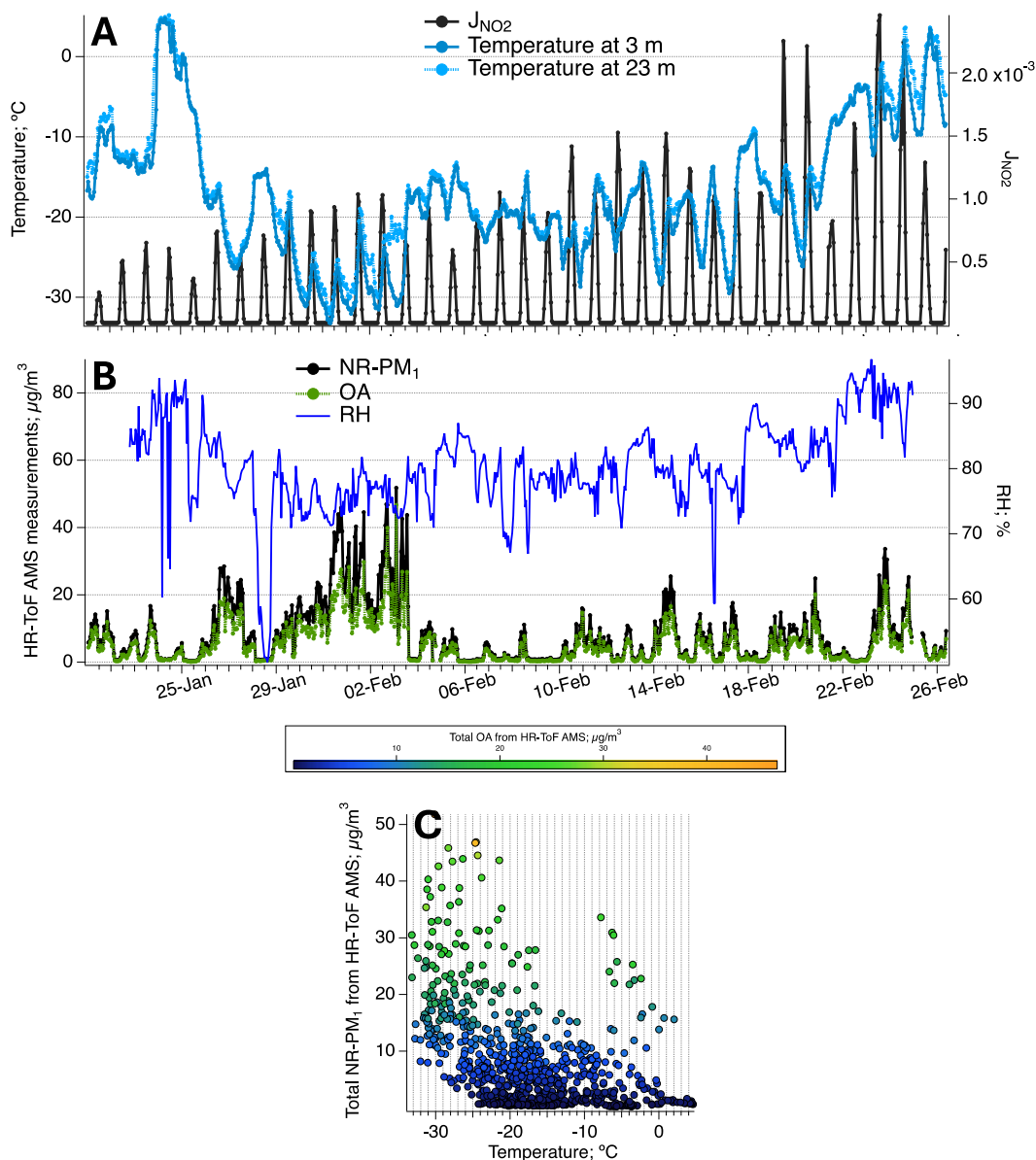


Figure S1 Overview of meteorological parameters and aerosol concentration during the ALPACA campaign, (A) Ambient temperature at 3 and 23 m and the daily sunlight in terms of the NO₂ photolysis rate coefficient (J_{NO_2}), (B) hourly concentrations of non-refractory fine particulate matter (NR-PM₁) and organic aerosol (OA) from the HR-ToF AMS, as well as relative humidity (RH), and (C) Hourly average NR-PM₁ and OA concentrations as a function of temperature.

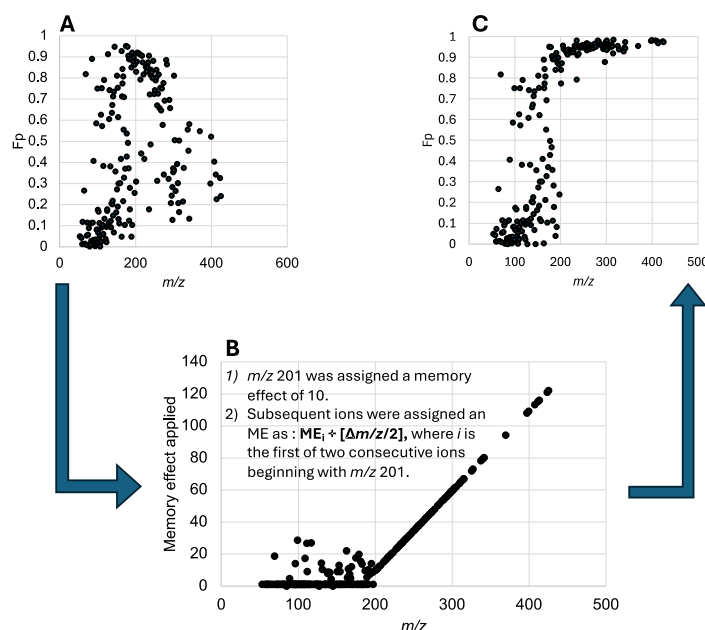


Figure S2 Overview of the error introduced due to the memory effect (ME) of switching the PTR-ToF MS from the gas phase to the particle phase. This memory effect was especially severe for ions with $m/z \geq 201$ and was corrected using an artificially increasing ME assigned based on m/z .

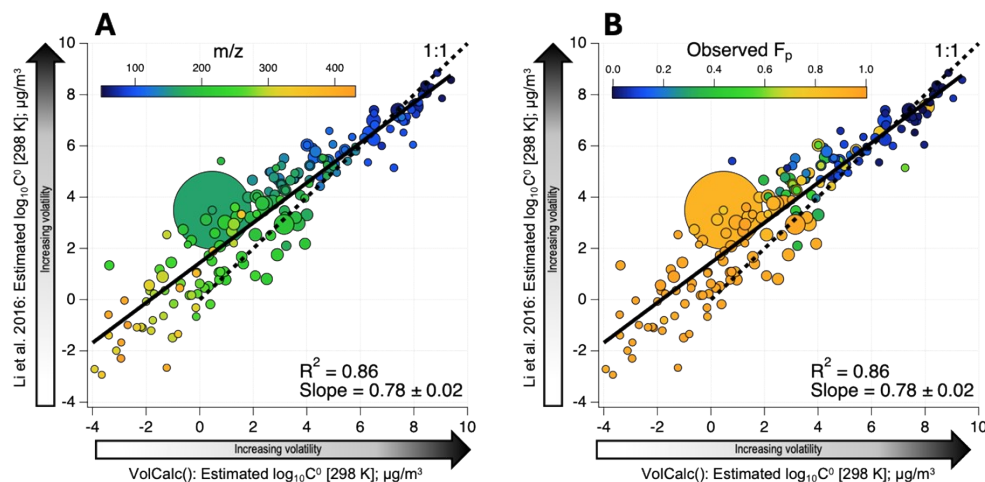


Figure S3 Comparison of the methods for the estimation of saturation mass concentrations (C^0) using the tentative identities given to the ions detected in PTR_{CHARON} analysis. The dependence of C^0 on (A) m/z and (B) observed F_p is also shown through the colours of the data points. Data points are sized by abundance normalised to the concentration of levoglucosan.

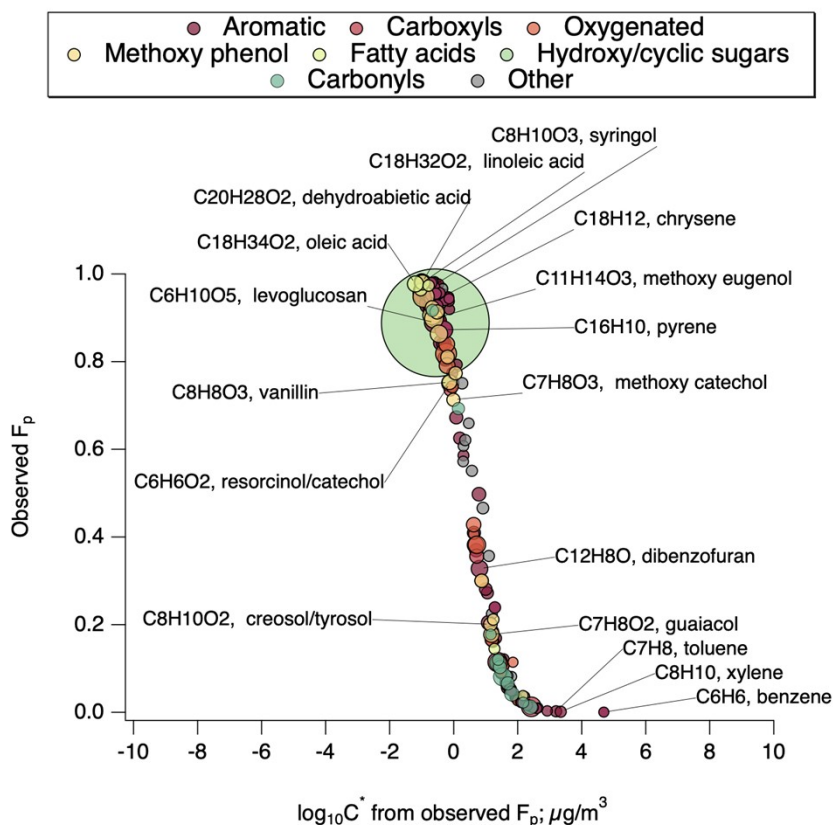


Figure S4. Campaign average F_p value during ALPACA campaign plotted against their logarithmic saturation concentrations calculated at the averaged measured temperature during the whole campaign. Only a small subset of the measured compounds is labelled.

References

1. Y. Peng, H. Wang, Y. Gao, S. Jing, S. Zhu, D. Huang, P. Hao, S. Lou, T. Cheng and C. Huang, *Atmospheric Measurement Techniques*, 2023, **16**, 15-28.
2. L. K. Meredith, S. M. Ledford, K. Riemer, P. Geffre, K. Graves, L. K. Honeker, D. LeBauer, M. M. Tfaily and J. Krechmer, *Frontiers in Microbiology*, 2023, **14**, 1267234.
3. J. F. Pankow and W. E. Asher, *Atmospheric Chemistry and Physics*, 2008, **8**, 2773-2796.
4. N. M. Donahue, A. Robinson, C. Stanier and S. Pandis, *Environmental science & technology*, 2006, **40**, 2635-2643.
5. H. Stark, R. L. Yatavelli, S. L. Thompson, H. Kang, J. E. Krechmer, J. R. Kimmel, B. B. Palm, W. Hu, P. L. Hayes and D. A. Day, *Environmental science & technology*, 2017, **51**, 8491-8500.
6. Y. Li, U. Pöschl and M. Shiraiwa, *Atmospheric Chemistry and Physics*, 2016, **16**, 3327-3344.
7. W.-S. W. DeRieux, Y. Li, P. Lin, J. Laskin, A. Laskin, A. K. Bertram, S. A. Nizkorodov and M. Shiraiwa, *Atmospheric Chemistry and Physics*, 2018, **18**, 6331-6351.

8. M. Shiraiwa, Y. Li, A. P. Tsimpidi, V. A. Karydis, T. Berkemeier, S. N. Pandis, J. Lelieveld, T. Koop and U. Pöschl, *Nature communications*, 2017, **8**, 1-7.
9. S. A. Epstein, I. Riipinen and N. M. Donahue, *Environmental science & technology*, 2010, **44**, 743-748.
10. H. E. Pence and A. Williams, *Journal of Chemical Education.*, 2010, **87**, 1123–1124.
11. M. Bilde, K. Barsanti, M. Booth, C. D. Cappa, N. M. Donahue, E. U. Emanuelsson, G. McFiggans, U. K. Krieger, C. Marcolli and D. Topping, *Chemical reviews*, 2015, **115**, 4115-4156.